UNIVERSITY OF AMSTERDAM

UvA-DARE (Digital Academic Repository)

A precision measurement of the number of neutrino species

Adeva, B.; Adriani, O.; Aguilar-Benitez, M.; Akbari, H.; Alcaraz, J.; Aloisio, A.; Alverson, G.; Alviggi, M.G.; Linde, F.L.

DOI
10.1016/0370-2693(90)91267-F

Publication date
1990

Published in
Physics Letters B

Link to publication

Citation for published version (APA):
Adeva, B., Adriani, O., Aguilar-Benitez, M., Akbari, H., Alcaraz, J., Aloisio, A., Alverson, G., Alviggi, M. G., & Linde, F. L. (1990). A precision measurement of the number of neutrino species. *Physics Letters B*, *249*, 341-352. https://doi.org/10.1016/0370-2693(90)91267-F

General rights
It is not permitted to download or to forward/distribute the text or part of it without the consent of the author(s) and/or copyright holder(s), other than for strictly personal, individual use, unless the work is under an open content license (like Creative Commons).

Disclaimer/Complaints regulations
If you believe that digital publication of certain material infringes any of your rights or (privacy) interests, please let the Library know, stating your reasons. In case of a legitimate complaint, the Library will make the material inaccessible and/or remove it from the website. Please Ask the Library: https://uba.uva.nl/en/contact, or a letter to: Library of the University of Amsterdam, Secretariat, Singel 425, 1012 WP Amsterdam, The Netherlands. You will be contacted as soon as possible.

UvA-DARE is a service provided by the library of the University of Amsterdam (https://dare.uva.nl)

Download date:03 Dec 2021

A precision measurement of the number of neutrino species

L3 Collaboration

B. Adeva [a], O. Adriani [b], M. Aguilar-Benitez [c], H. Akbari [d], J. Alcaraz [c], A. Aloisio [e], G. Alverson [f], M.G. Alviggi [e], Q. An [g], H. Anderhub [h], A.L. Anderson [i], V.P. Andreev [j], T. Angelov [i], L. Antonov [k], D. Antreasyan [l], P. Arce [c], A. Arefiev [m], T. Azemoon [n], T. Aziz [o], P.V.K.S. Baba [g], P. Bagnaia [p], J.A. Bakken [q], L. Baksay [r], R.C. Ball [n], S. Banerjee [o, g], J. Bao [d], L. Barone [p], A. Bay [s], U. Becker [i], J. Behrens [h], S. Beingessner [t], Gy.L. Bencze [u, r], J. Berdugo [c], P. Berges [i], B. Bertucci [p], B.L. Betev [k], A. Biland [h], R. Bizzarri [p], J.J. Blaising [t], P. Blömeke [v], B. Blumenfeld [d], G.J. Bobbink [w], M. Bocciolini [b], W. Böhlen [x], A. Böhm [v], T. Böhringer [y], B. Borgia [p], D. Bourilkov [k], M. Bourquin [s], D. Boutigny [t], J.G. Branson [z], I.C. Brock [α], F. Bruyant [a], C. Buisson [β], A. Bujak [γ], J.D. Burger [i], J.P. Burq [β], J. Busenitz [δ], X.D. Cai [g], C. Camps [v], M. Capell [n], F. Carbonara [e], F. Carminati [b], A.M. Cartacci [b], M. Cerrada [c], F. Cesaroni [p], Y.H. Chang [i], U.K. Chaturvedi [g], M. Chemarin [β], A. Chen [ε], C. Chen [ζ], G.M. Chen [ζ], H.F. Chen [η], H.S. Chen [ζ], M. Chen [i], M.L. Chen [n], G. Chiefari [e], C.Y. Chien [d], C. Civinini [b], I. Clare [i], R. Clare [i], G. Coignet [t], N. Colino [a], V. Commichau [v], G. Conforto [b], A. Contin [a], F. Crijns [w], X.Y. Cui [g], T.S. Dai [i], R. D'Alessandro [b], R. de Asmundis [e], A. Degré [t], K. Deiters [a, θ], E. Dénes [u], P. Denes [q], F. DeNotaristefani [p], M. Dhina [h], D. DiBitonto [δ], M. Diemoz [p], F. Diez-Hedo [a], H.R. Dimitrov [k], C. Dionisi [p], F. Dittus [κ], R. Dolin [i], E. Drago [e], T. Driever [w], D. Duchesneau [s], P. Duinker [w, a], I. Duran [a, c], H. El Mamouni [β], A. Engler [α], F.J. Eppling [i], F.C. Erné [w], P. Extermann [s], R. Fabbretti [h], G. Faber [i], S. Falciano [a, p], Q. Fan [g, ζ], S.J. Fan [λ], M. Fabre [h], J. Fay [β], J. Fehlmann [h], H. Fenker [f], T. Ferguson [α], G. Fernandez [c], F. Ferroni [p, a], H. Fesefeldt [v], J. Field [s], G. Finocchiaro [p], P.H. Fisher [d], G. Forconi [s], T. Foreman [w], K. Freudenreich [h], W. Friebel [θ], M. Fukushima [i], M. Gailloud [y], Yu. Galaktionov [m], E. Gallo [b], S.N. Ganguli [o], P. Garcia-Abia [c], S.S. Gau [ε], S. Gentile [p], M. Gettner [f], M. Glaubman [f], S. Goldfarb [n], Z.F. Gong [g, η], E. Gonzalez [c], A. Gordeev [m], P. Göttlicher [v], D. Goujon [s], C. Goy [t], G. Gratta [κ], A. Grimes [f], C. Grinnell [i], M. Gruenewald [κ], M. Guanziroli [g], A. Gurtu [o], L.J. Gutay [γ], H. Haan [v], S. Hancke [v], K. Hangarter [v], M. Harris [a], A. Hasan [g], C.F. He [λ], A. Heavey [q], T. Hebbeker [v], M. Hebert [z], G. Herten [i], U. Herten [v], A. Hervé [a], K. Hilgers [v], H. Hofer [h], H. Hoorani [g], L.S. Hsu [ε], G. Hu [g], G.Q. Hu [λ], B. Ille [β], M.M. Ilyas [g], V. Innocente [c, a], E. Isiksal [h], E. Jagel [g], B.N. Jin [ζ], L.W. Jones [n], P. Kaaret [q], R.A. Khan [g], Yu. Kamyshkov [m], D. Kaplan [f], Y. Karyotakis [t, a], M. Kaur [g], S. Khokhar [g], V. Khoze [j], D. Kirkby [κ], W. Kittel [w], A. Klimentov [m], A.C. König [w], O. Kornadt [v], V. Koutsenko [m], R.W. Kraemer [α], T. Kramer [i], V.R. Krastev [k], W. Krenz [v], J. Krizmanic [d], A. Kuhn [x], K.S. Kumar [μ], V. Kumar [g], A. Kunin [m], S. Kwan [f], A.van Laak [v], V. Lalieu [s], G. Landi [b], K. Lanius [a, θ], W. Lange [θ], D. Lanske [v], S. Lanzano [e], P. Lebrun [β], P. Lecomte [h], P. Lecoq [a], P. Le Coultre [h], I. Leedom [f], J.M. Le Goff [a], A. Leike [θ], L. Leistam [a], R. Leiste [θ], J. Lettry [h], P.M. Levchenko [j], X. Leytens [w], C. Li [η], H.T. Li [ζ], J.F. Li [g], L. Li [h], P.J. Li [λ], Q. Li [g], X.G. Li [ζ], J.Y. Liao [λ], Z.Y. Lin [η], F.L. Linde [α], D. Linnhofer [a], R. Liu [g], Y. Liu [g], W. Lohmann [θ], S. Lökös [r], E. Longo [p], Y.S. Lu [ζ], J.M. Lubbers [w], K. Lübelsmeyer [v], C. Luci [a], D. Luckey [g, i], L. Ludovici [p], X. Lue [h], L. Luminari [p], W.G. Ma [η], M. MacDermott [h], R. Magahiz [r], M. Maire [t], P.K. Malhotra [o], R. Malik [g], A. Malinin [m], C. Maña [a, c], D.N. Mao [n], Y.F. Mao [ζ], M. Maolinbay [h], P. Marchesini [g], A. Marchionni [b], J.P. Martin [β], L. Martinez [c], F. Marzano [p],

0370-2693/90/$ 03.50 © 1990 – Elsevier Science Publishers B.V. (North-Holland)

G.G.G. Massaro [w], T. Matsuda [i], K. Mazumdar [o], P. McBride [μ], T. McMahon [γ], D. McNally [h], Th. Meinholz [v], M. Merk [w], L. Merola [e], M. Meschini [b], W.J. Metzger [w], Y. Mi [g], M. Micke [v], U. Micke [v], G.B. Mills [n], Y. Mir [g], G. Mirabelli [p], J. Mnich [v], M. Möller [v], L. Montanet [a], B. Monteleoni [b], G. Morand [s], R. Morand [t], S. Morganti [p], V. Morgunov [m], R. Mount [κ], E. Nagy [u, a], M. Napolitano [e], H. Newman [κ], M.A. Niaz [g], L. Niessen [v], W.D. Nowak [θ], H. Nowak [θ], S. Nowak [θ], D. Pandoulas [v], G. Paternoster [e], S. Patricelli [c], Y.J. Pei [v], D. Perret-Gallix [t], J. Perrier [s], A. Pevsner [d], M. Pieri [b], P.A. Piroué [q], V. Plyaskin [m], M. Pohl [h], V. Pojidaev [m], N. Produit [s], J.M. Qian [i, g], K.N. Qureshi [g], R. Raghavan [o], G. Rahal-Callot [h], P. Razis [h], K. Read [q], D. Ren [h], Z. Ren [g], S. Reucroft [f], T. Riemann [θ], C. Rippich [α], H.A. Rizvi [g], B.P. Roe [n], M. Röhner [v], S. Röhner [v], Th. Rombach [v], L. Romero [c], J. Rose [v], S. Rosier-Lees [t], R. Rosmalen [w], Ph. Rosselet [y], J.A. Rubio [a, c], W. Ruckstuhl [s], H. Rykaczewski [h], M. Sachwitz [θ], J. Salicio [c], J.M. Salicio [c], G. Sartorelli [ℓ, g], G. Sauvage [t], A. Savin [m], V. Schegelsky [j], D. Schmitz [v], P. Schmitz [v], M. Schneegans [t], M. Schöntag [v], H. Schopper [ξ], D.J. Schotanus [w], H.J. Schreiber [θ], R. Schulte [v], S. Schulte [v], K. Schultze [v], J. Schütte [μ], J. Schwenke [v], G. Schwering [v], C. Sciacca [e], R. Sehgal [g], P.G. Seiler [h], J.C. Sens [w], I. Sheer [z], V. Shevchenko [m], S. Shevchenko [m], X.R. Shi [α], K. Shmakov [m], V. Shoutko [m], E. Shumilov [m], N. Smirnov [j], A. Sopczak [κ, z], C. Souyri [t], C. Spartiotis [d], T. Spickermann [v], B. Spiess [x], P. Spillantini [b], R. Starosta [v], M. Steuer [ℓ, i], D.P. Stickland [q], B. Stöhr [h], H. Stone [s], K. Strauch [μ], B.C. Stringfellow [γ], K. Sudhakar [o, v], G. Sultanov [a], R.L. Sumner [q], H. Suter [h], R.B. Sutton [α], J.D. Swain [g], A.A. Syed [g], X.W. Tang [ζ], E. Tarkovsky [m], J.M. Thenard [t], E. Thomas [g], C. Timmermans [w], Samuel C.C. Ting [i], S.M. Ting [i], Y.P. Tong [e], F. Tonisch [θ], M. Tonutti [v], S.C. Tonwar [o], J. Tòth [u], G. Trowitzsch [θ], K.L. Tung [ζ], J. Ulbricht [x], L. Urbàn [u], U. Uwer [v], E. Valente [p], R.T. Van de Walle [w], H. van der Graaf [w], I. Vetlitsky [m], G. Viertel [h], P. Vikas [g], U. Vikas [g], M. Vivargent [t, i], H. Vogel [α], H. Vogt [θ], M. Vollmar [v], G. Von Dardel [a], I. Vorobiev [m], A.A. Vorobyov [j], An.A. Vorobyov [j], L. Vuilleumier [y], M. Wadhwa [g], W. Walk [a], W. Wallraff [v], C.R. Wang [η], G.H. Wang [α], J.H. Wang [ζ], Q.F. Wang [μ], X.L. Wang [η], Y.F. Wang [b], Z. Wang [g], Z.M. Wang [g, η], J. Weber [h], R. Weill [y], T.J. Wenaus [i], J. Wenninger [s], M. White [i], R. Wilhelm [w], C. Willmott [c], F. Wittgenstein [a], D. Wright [q], R.J. Wu [ζ], S.L. Wu [g], S.X. Wu [g], Y.G. Wu [ζ], B. Wysłouch [i, a], Z.Z. Xu [η], Z.L. Xue [λ], D.S. Yan [λ], B.Z. Yang [η], C.G. Yang [ζ], G. Yang [g], K.S. Yang [ζ], Q.Y. Yang [ζ], Z.Q. Yang [λ], Q. Ye [g], C.H. Ye [g], S.C. Yeh [ε], Z.W. Yin [λ], J.M. You [g], C. Zabounidis [f], C. Zaccardelli [κ], L. Zehnder [h], M. Zeng [g], Y. Zeng [v], D. Zhang [z], D.H. Zhang [w], S.Y. Zhang [ζ], Z.P. Zhang [η], J.F. Zhou [v], R.Y. Zhu [κ], A. Zichichi [a, g] and J. Zoll [a]

[a] *European Laboratory for Particle Physics, CERN, CH-1211 Geneva 23, Switzerland*
[b] *INFN – Sezione di Firenze and University of Firenze, I-50125 Florence, Italy*
[c] *Centro de Investigaciones Energeticas, Medioambientales y Tecnologicas, CIEMAT, E-28040 Madrid, Spain*
[d] *Johns Hopkins University, Baltimore, MD 21218, USA*
[e] *INFN – Sezione di Napoli and University of Naples, I-80125 Naples, Italy*
[f] *Northeastern University, Boston, MA 02115, USA*
[g] *World Laboratory, FBLJA Project, CH-1211 Geneva, Switzerland*
[h] *Eidgenössische Technische Hochschule, ETH Zürich, CH-8093 Zurich, Switzerland*
[i] *Massachusetts Institute of Technology, Cambridge, MA 02139, USA*
[j] *Leningrad Nuclear Physics Institute, SU-188 350 Gatchina, USSR*
[k] *Central Laboratory of Automation and Instrumentation, CLANP, Sofia, Bulgaria*
[ℓ] *INFN – Sezione di Bologna, I-40126 Bologna, Italy*
[m] *Institute of Theoretical and Experimental Physics, ITEP, SU-117 259 Moscow, USSR*
[n] *University of Michigan, Ann Arbor, MI 48109, USA*
[o] *Tata Institute of Fundamental Research, Bombay 400 005, India*
[p] *INFN – Sezione di Roma and University of Rome "La Sapienza", I-00185 Rome, Italy*
[q] *Princeton University, Princeton, NJ 08544, USA*
[r] *Union College, Schenectady, NY 12308, USA*
[s] *University of Geneva, CH-1211 Geneva 4, Switzerland*

[t] Laboratoire de Physique des Particules, LAPP, F-74519 Annecy-le-Vieux, France
[u] Central Research Institute for Physics of the Hungarian Academy of Sciences, H-1525 Budapest 114, Hungary
[v] I. Physikalisches Institut, RWTH, D-5100 Aachen, FRG [1]
and III. Physikalisches Institut, RWTH, D-5100 Aachen, FRG [1]
[w] National Institute for High Energy Physics, NIKHEF, NL-1009 DB Amsterdam, The Netherlands
and NIKHEF-H and University of Nijmegen, NL-6525 ED Nijmegen, The Netherlands
[x] Paul Scherrer Institut (PSI), Würenlingen, Switzerland
[y] University of Lausanne, CH-1015 Lausanne, Switzerland
[z] University of California, San Diego, CA 92182, USA
[α] Carnegie Mellon University, Pittsburgh, PA 15213, USA
[β] Institut de Physique Nucléaire de Lyon, IN2P3-CNRS/Université Claude Bernard, F-69622 Villeurbanne Cedex, France
[γ] Purdue University, West Lafayette, IN 47907, USA
[δ] University of Alabama, Tuscaloosa, AL 35486, USA
[ε] High Energy Physics Group, Taiwan, ROC
[ζ] Institute of High Energy Physics, IHEP, Beijing, P.R. China
[η] Chinese University of Science and Technology, USTC, Hefei, Anhui 230 029, P.R. China
[θ] High Energy Physics Institute, DDR-1615 Zeuthen-Berlin, GDR
[κ] California Institute of Technology, Pasadena, CA 91125, USA
[λ] Shanghai Institute of Ceramics, SIC, Shanghai, P.R. China
[μ] Harvard University, Cambridge, MA 02139, USA
[ξ] University of Hamburg, D-2000 Hamburg, FRG

Received 19 July 1990

We have measured the cross section for $e^+e^- \to$ hadrons over the center of mass energy range of the Z^0 peak, from 88.22 to 95.03 GeV. We determine the Z^0 mass $M_Z = 91.164 \pm 0.013$(experiment) ± 0.030(LEP) GeV. Within the framework of the standard model we determine the invisible width, $\Gamma_{\text{invisible}} = 0.502 \pm 0.018$ GeV, and the number of light neutrino species, $N_\nu = 3.01 \pm 0.11$. We exclude the existence of a supersymmetric scalar neutrino having a mass less than 31.4 GeV, at the 95% confidence level. We performed a model independent combined fit to the $e^+e^- \to$ hadrons and $e^+e^- \to \mu^+\mu^-$ data to determine total width, leptonic width and hadronic width of the Z^0.

1. Introduction

Accurate measurements of the cross sections for $e^+e^- \to$ hadrons and $e^+e^- \to$ leptons in the mass region of the neutral intermediate vector boson Z^0 are important in providing a precise determination of the Z^0 properties, and of the number of light neutrino species. The predictions of the standard electroweak model [1], and their internal consistency, can also be tested with higher sensitivity by combining measurements of hadronic decays and leptonic decays.

We report on data collected at center of mass energies covering the range of the Z^0 peak: 88.22 GeV $\leqslant \sqrt{s} \leqslant$ 95.03 GeV, with the L3 detector at LEP. A standard model fit to the cross sections of $e^+e^- \to$ hadrons reaction is used to make a precise determination of the number of neutrino flavors. We also report on a model independent fit to the $e^+e^- \to$ hadrons and the $e^+e^- \to \mu^+\mu^-$ data to determine the Z^0 properties, including the width $\Gamma_{\text{invisible}}$ to all unobserved final states. For this fit, only lepton universality is assumed with a lineshape given by a Breit–Wigner resonance with an energy-dependent width. Earlier measurements of Z^0 properties may be found in refs. [2,3].

We have increased our statistics by a factor of five over our previous analysis [2]. Due to improved detector performance, improved calibrations and the use of redundant triggers we are able to reduce substantially the systematic errors on our hadron and luminosity measurements.

2. The L3 detector and the data samples

The L3 detector covers 99% of 4π. The detector includes a central vertex chamber, a precise electromagnetic calorimeter composed of BGO crystals, a uranium and brass hadron calorimeter with proportional wire chamber readout, a high accuracy muon

chamber system, and a ring of scintillation counters. These detectors are installed in a 12 m inner diameter magnet which provides a uniform field of 0.5 T along the beam direction. The luminosity is determined by measuring small angle Bhabha events in two forward calorimeters consisting of BGO crystals. A detailed description of each detector subsystem, and its performance, are given in ref. [4].

For the present analysis, we used the data collected in the following ranges of polar angles:

- for the hadron calorimeter, $5° < \theta < 175°$,
- for the muon chambers, $35.8° < \theta < 144.2°$,
- for the electromagnetic calorimeter, $42.4° < \theta < 137.6°$.

Data from the 1989 (October–December) and the 1990 (March–June) LEP running periods are included. The 1989 data have been published [2]. We describe in this paper the analysis of the 1990 data.

3. Measurement of luminosity

The luminosity is measured by eight radial layers of BGO crystals at small angles, situated on either side of the interaction point. The energy resolution of these calorimeters is dominated by the calibration accuracy, and is typically 2%. The θ and ϕ impact coordinates of the electron and positron are determined from the observed energy sharing among the crystals, and from a fitting function derived from the known average shape of electromagnetic showers. Using this technique, the energy of the incident particle is also corrected for lateral losses.

The Bhabha event candidates must satisfy one of the following two trigger conditions: (A) Back-to-back coincidence with $\geqslant 15$ GeV in each forward BGO calorimeter. (B) Coincidence between $\geqslant 25$ GeV in one forward BGO calorimeter and $\geqslant 5$ GeV in the other. The trigger efficiency is determined to be $(99.7 \pm 0.1)\%$ by using a prescaled "single tag" trigger which required $\geqslant 30$ GeV in only one of the two forward BGO calorimeters.

We used the following cuts to select the Bhabha event candidates:

(1) $|\Delta\phi - 180°| < 10°$,

(2) $\max(E_1, E_2) > \frac{4}{5}E_{\text{Beam}}$ and $\min(E_1, E_2) > \frac{2}{5}E_{\text{Beam}}$,

(3) 30.92 mrad $\leqslant \theta_1 \leqslant$ 64.41 mrad and 24.93 mrad $\leqslant \theta_2 \leqslant$ 69.94 mrad,

where $\Delta\phi$ is the coplanarity angle between the electron and positron, and $\theta_{1,2}$, $E_{1,2}$ are their polar angles and energies, respectively. Cut (3) requires that one particle enters a small fiducial region (crystal layers 2–7) on either side of the interaction point, and the second particle enters a larger fiducial region (crystal layers 1–8) on the opposite side. Two event samples are selected. In the first sample, the smaller fiducial region is imposed on the forward BGO calorimeter on electron side, while in the second sample the smaller fiducial region is imposed on the calorimeter on the positron side. The number of events used to calculate the luminosity is the average of the number of events in the two samples. This method reduces the systematic effect of offsets of up to 2 mm in position and 1 mrad in angle of the calorimeters relative to the beam line to the 0.1% level. We correct for the background on a run-by-run basis using sidebands of the coplanarity distribution. The average background level of 0.7% consists in almost equal proportion of coincidences of beam–gas interactions and radiative Bhabha events.

To determine the acceptance, $e^+e^- \to e^+e^-(\gamma)$ events are generated at the Z^0 pole using the BABAMC Monte Carlo program [5]. The generated events are passed through the L3 detector simulation program [6], which includes the effects of energy loss, multiple scattering and showering in the detector materials and the beam pipe. The simulated events are analyzed by the same program used to analyze the data. The cross section within our acceptance is corrected for the contamination from the $e^+e^- \to \gamma\gamma(\gamma)$ process (0.02%) [7] and for the $e^+e^- \to Z^0 \to e^+e^-$ contribution (up to 0.2% for off peak center of mass energies) [8].

The systematic uncertainty in the cross section within our acceptance includes contributions from Monte Carlo statistics (0.6%) and internal detector geometry (0.6%). The crucial geometric variable is the minimum accepted Bhabha scattering angle, $\theta_{\min}$. From survey measurements we determine $\theta_{\min} = 30.92 \pm 0.09$ mrad. Independently, we obtain $\theta_{\min} = 30.94 \pm 0.03(\text{stat}) \pm 0.09(\text{syst})$ mrad from the precision proportional chambers mounted in front of the forward BGO calorimeters. The theoretical uncertainty, resulting from the approximations in the cal-

culation used in BABAMC and the effect of higher order terms, is estimated to be 0.7%. Adding these numbers in quadrature, we obtain an overall systematic uncertainty in the cross section of 1.1%.

The effect on the integrated luminosity, $\mathscr{L}$, of changes in the Bhabha event selection is shown in figs. 1a–1c. The value of $\mathscr{L}$ is stable against changes in the coplanarity and/or the energy cut. They are all consistent with zero change. Removal of successive crystal layers of the smaller fiducial volume reduces the Bhabha sample substantially. This explains the large statistical uncertainty in fig. 1c on the changes in the fiducial volume cut. By adding in quadrature the changes in $\mathscr{L}$ for each cut, we estimate a systematic error in $\mathscr{L}$ due to our event selection of 0.7%.

Combining in quadrature the systematic uncertainties in the trigger efficiency (0.1%), in the cross section (1.1%) and in the event selection (0.7%), we obtain a total systematic uncertainty in the luminosity of 1.3%.

In fig. 2a the measured coplanarity distribution, before the $|\Delta\phi - 180°| < 10°$ cut, is compared to the Monte Carlo prediction. In figs. 2b, 2c the measured E/E_{Beam} and $dN/d\theta$ distributions for the final selected Bhabha sample are shown together with their Monte Carlo predictions. All three distributions are in good agreement with the Monte Carlo simulation. The number of Bhabha events and the corresponding integrated luminosity for each center of mass energy are listed in table 1.

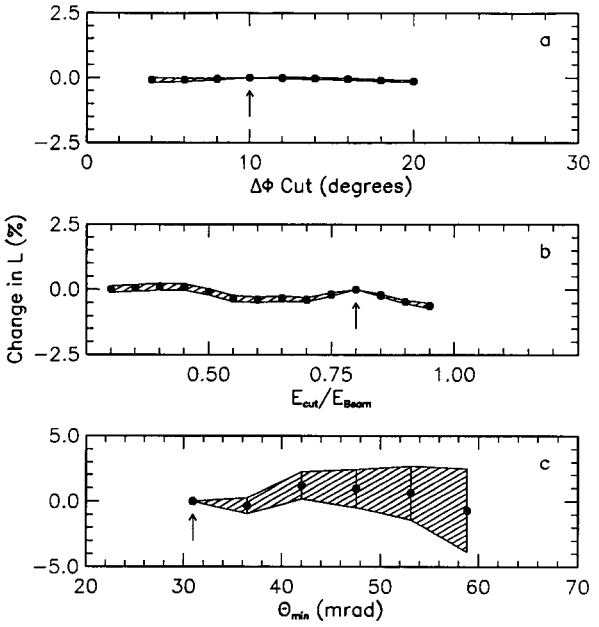

Fig. 1. The relative change in the integrated luminosity as a function of (a) the coplanarity cut $\Delta\phi$, (b) the energy cut $E_{\text{cut}}/E_{\text{Beam}}$ and (c) the smaller fiducial volume cut θ_{min}. The shaded region in each plot represents the $\pm 1\sigma$ contour and the arrows indicate the standard cut values.

4. Monte Carlo programs for Bhabha scattering

There is good agreement between our measured E, θ and $\Delta\phi$ distributions and the corresponding Monte Carlo predictions from either the BABAMC or BHLUMI V1.2 [9] programs. In our 1989 luminosity analysis we used the BHLUMI V1.2 Monte Carlo program, which generates multiple radiated photons, to determine the $e^+e^- \to e^+e^-(\gamma)$ cross section within our acceptance. The BHLUMI program can only generate events with scattered $e^{\pm}$ energies larger than xE_{Beam}, with $x > 0.4$ [9]. Our luminosity monitor does not differentiate an $e^{\pm}$ from a γ. We therefore correct the cross section for the omission of hard photon radiation ($x \leqslant 0.4$) using the BABAMC Monte Carlo program. This correction factor is a monotonically increasing function of x. During the study of luminosity for our 1990 data, we found that the BHLUMI V1.2 cross section within our acceptance has an unphysical maximum around $x = 0.5$. This leads us to use the BABAMC Monte Carlo program rather than BHLUMI for our current acceptance calculation.

The cross section within our acceptance from BHLUMI V1.2, corrected for hard photon emission, and that from BABAMC differ by $-(4 \pm 1)\%$. A more accurate Yennie–Frautschi–Suura form factor [10] and a better vacuum polarization function implemented in BHLUMI V1.11, reduces this difference to $-(2 \pm 1)\%$. However, the BHLUMI V1.11 cross section still has an unphysical maximum around $x = 0.5$.

In table 1, lower part, the integrated luminosities rescaled by 0.96 are listed for each center of mass energy of our 1989 data sample.

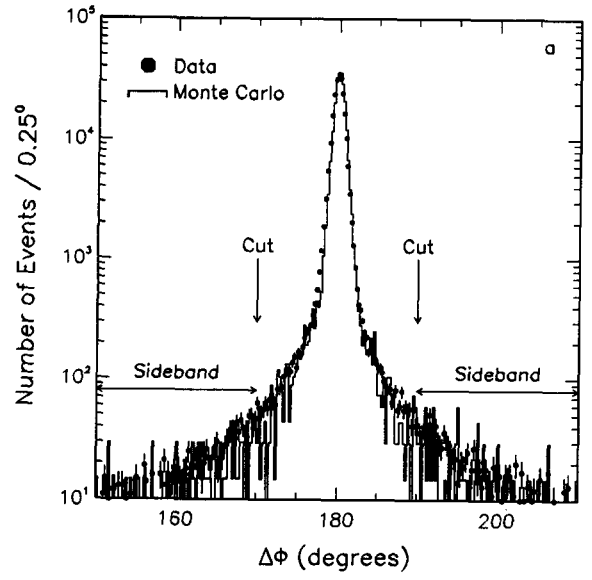

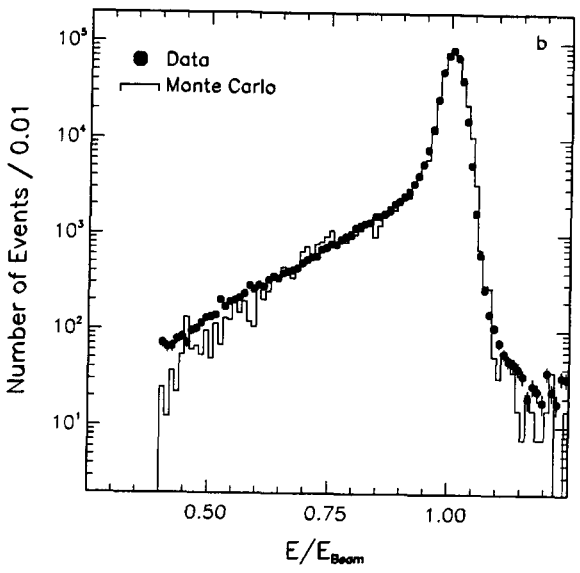

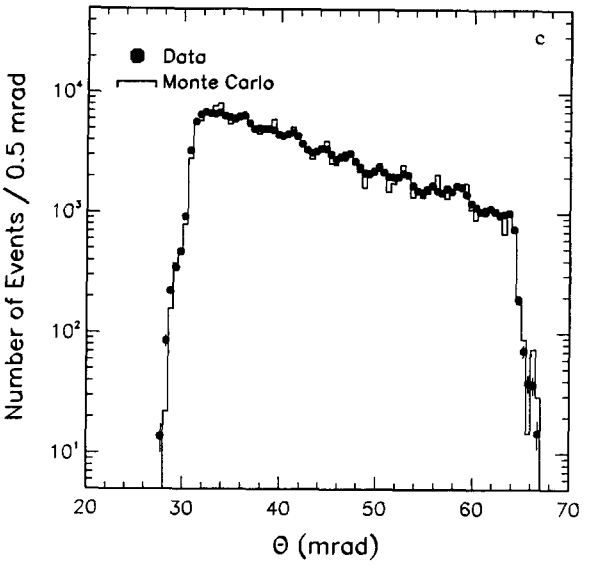

Fig. 2. (a) The observed coplanarity distribution $\Delta\phi$ compared to the Monte Carlo simulation for Bhabha event candidates. The cuts used to select Bhabha events, $|\Delta\phi - 180°| < 10°$, and the sidebands used for the background correction are indicated in the figure. (b) Distribution of the observed $e^{\pm}$ energies normalized to the beam energy compared to the Monte Carlo simulation for Bhabha events. (c) Distribution of the observed polar scattering angle, θ, compared to the Monte Carlo simulation for Bhabha events. The wiggles in the distributions are due to the changing angular resolution across the face of each crystal. Number of events used for data and Monte Carlo are 220×10^3 and 15×10^3, respectively.

5. Triggers for hadron events

The primary trigger used for hadronic events in this analysis requires either a total energy of 15 GeV in the barrel region of the calorimeters ($|\cos\theta| < 0.74$) or 20 GeV in the whole detector. For the data collected in 1990 (approximately 80% of the total) this trigger was put into a logical OR with two other triggers: a scintillator trigger requiring at least five of the sixteen scintillation counters to have fired, and a charged track trigger requiring two tracks in approximately opposite ϕ-sectors of the central vertex chamber. An analysis of the accepted hadronic events showed that the calorimetric trigger is $(99.95 \pm 0.05)\%$ efficient, and the scintillation counter and track triggers are each 95% efficient. The total systematic error due to trigger inefficiencies is negligible.

Table 1
Measured cross section, σ_h, for $e^+e^- \to$ hadrons.

	$\sqrt{s}$ (GeV)	Hadron events	Bhabha events	Luminosity (nb^{-1})	σ_h (nb)
1990	88.227	493	11406	109.16	4.62 ± 0.21
	89.224	1912	23524	230.35	8.55 ± 0.20
	90.224	4196	23006	230.35	18.63 ± 0.31
	91.223	36389	119239	1219.97	30.50 ± 0.18
	92.222	3116	14049	147.60	21.59 ± 0.43
	93.222	2006	15987	171.68	11.95 ± 0.28
	94.219	1098	12721	138.95	8.07 ± 0.25
	ALL	49219	219932	2247.31	
1989	88.279	207	3565	40.5	5.45 ± 0.40
	89.277	521	5397	62.8	8.76 ± 0.41
	90.277	993	4389	52.3	19.77 ± 0.70
	91.030	2284	6492	78.6	30.41 ± 0.74
	91.278	3351	8776	116.3	30.30 ± 0.62
	91.529	3352	9742	119.0	29.62 ± 0.59
	92.280	897	3293	44.8	20.82 ± 0.79
	93.276	595	3977	49.2	12.56 ± 0.55
	94.278	193	2241	28.9	7.17 ± 0.54
	95.036	72	810	10.7	7.04 ± 0.86
	ALL	12465	48682	603.1	

6. Event selection and acceptance for hadronic events

The events from the process $e^+e^- \to$ hadrons are selected and analyzed by two independent teams of physicists. Each team uses its own event selection criteria and cuts (one set of criteria is described in detail below). The two event samples obtained differ by 1%, and the acceptances for hadronic events (97.8% and 96.7%, respectively) vary by 1% in the same direction, resulting in a difference in the calculated cross sections of less than 0.25%. The agreement in the event samples and cross sections gives us added confidence in the validity of the results and in the systematic errors which we quote.

The event selections are based on the energy measured in the electromagnetic and hadron calorimeters, and the momentum of any muons measured in the muon chambers. The Monte Carlo distributions are generated by the LUND parton shower program, JETSET 7.2 [11]. The b quark fragmentation function is adjusted to match our measured inclusive muon data [12]. The generated events are passed through the L3 detector simulation [6]. After simulation, the events are analyzed by the same program used to analyze the data.

The hadronic events listed in table 1, upper part, are selected using the criteria

(1) $0.5 < E_{vis}/\sqrt{s} < 1.5$,

(2) $|E_\parallel|/E_{vis} < 0.37$,

(3) $E_\perp/E_{vis} < 0.37$,

where E_{vis} is the total energy observed in the detector, $E_\parallel$ is the energy imbalance along the beam direction, and $E_\perp$ is the transverse energy imbalance.

A clustering algorithm is used to group energy depositions in the calorimeters. The algorithm on average reconstructs only one cluster for each electron or photon shower, or muon, only a few clusters for τ's and about forty clusters for an hadronic event. Thus, we are able to reject e^+e^-, $\mu^+\mu^-$, and $\tau^+\tau^-$ events by a cut on the number of clusters. Since the granularity and the minimum energy needed to form a cluster in the endcaps is slightly larger than in the barrel region, we use two different cuts, the choice of cut being determined by the polar angle of the total event thrust axis:

(4a) $N_{cluster} > 10$ for $|\cos\theta| > 0.74$ (Endcap),

(4b) $N_{cluster} > 16$ for $|\cos\theta| < 0.74$ (Barrel).

Applying these cuts to a sample of simulated events,

we calculate an acceptance of $(97.8 \pm 0.1)\%$ (statistical error only) for hadronic decays of the Z^0. An analysis of simulated $\tau^+\tau^-$ and e^+e^- final states and a visual scan of the off-peak events, yield a net contamination in the hadronic event sample of $(0.04 \pm 0.02)\%$ and less than 0.15% (off-peak), respectively. The contribution to the event sample from the "two-photon process" $e^+e^- \to e^+e^- +$ hadrons is negligible.

The simulated distributions in the cut variables agree very closely with the corresponding distributions obtained for the real data. Fig. 3 shows that the data distributions in $E_{\mathrm{vis}}/\sqrt{s}$, $|E_{\mathrm{imb}}|/E_{\mathrm{vis}}$, where $|E_{\mathrm{imb}}|$ is the modulus of the vector sum of $E_{\parallel}$ and $E_{\perp}$, and the number of energy clusters (N_{cluster}) are in excellent agreement with the Monte Carlo predictions in the accepted regions.

Fig. 4 shows the effect on our final cross sections of varying the cuts over a wide range. On the basis of these plots, we are able to assign a total systematic error in the acceptance of 0.7%.

Visual scans of more than a thousand events confirm that the background in the hadronic event sample (i.e. events not from high energy e^+e^- interactions, such as beam–gas, beam–pipe interactions) is negligible.

Studies of the energy dependence of the acceptance, and of the ratio of the number of events collected versus integrated luminosity, as a function of time during the running periods, show no evidence of significant point-to-point systematic errors in our scan over the Z^0 peak.

We obtain an overall systematic error in the corrected number of hadronic events of 0.7%. Combining this error in quadrature with the 1.3% error on the luminosity, gives an overall systematic error on the measured hadronic cross sections 1.5%.

7. Event sample and cross sections for $e^+e^- \to$ hadrons

Table 1, upper part, lists the cross section for $e^+e^- \to$ hadrons as a function of the center of mass energy, along with the number of hadronic events, the number of Bhabha events, and the integrated luminosity at each energy point. The data shown are for the runs since our last publication [2]. The errors on the cross sections in the table do not include the overall systematic error of 1.5%.

The integrated luminosities and corresponding cross sections given in ref. [2] are scaled as described above. They are listed in table 1b, lower part. The overall systematic error for these data is 1.0% for the hadronic selection and 1.7% for the luminosity, giving a combined systematic error of 2.0% (not shown in the table).

The $\sqrt{s}$ values are provided by the LEP machine group. The absolute energy scale error is determined to be ± 30 MeV [13].

8. Determination of the number of neutrino species

The measured cross sections in the above tables are used to determine the values of M_Z and $\Gamma_{\mathrm{invisible}}$ using a fit within the framework of the standard model. This fit depends on the standard model calculation of Γ_{ee} and Γ_h, on the value of the strong coupling constant α_s, and on the masses of the top quark, M_t, and the Higgs, M_H. For these fits, we fixed $\alpha_s = 0.115$ [14], $M_H = 100$ GeV and $M_t = 150$ GeV, respectively. The effect on the fit results of varying these quantities is discussed below.

The data in tables 1a and 1b are fitted simultaneously using a common luminosity error given by the luminosity-weighted systematic errors. The overall luminosity error is 1.4%. The separate event selection systematic errors are also combined to give a common event selection systematic error of 0.8%.

We also perform fits to the 1989 and 1990 data separately and determine the parameters from the weighted average of the separate results. This procedure would be sensitive to any uncorrected absolute shifts in the LEP energy calibration between the two running periods. The results are completely consistent with the values given below.

Analytical forms for the Z^0 cross section are used in the fit [15–17]. These include initial state radiation and a Breit–Wigner shape for the resonance with an energy-dependent width. These programs produce identical fit results and cross sections in agreement with the standard model program [18], if the same values of the mass, width and branching ratios are used.

The results of the fit are

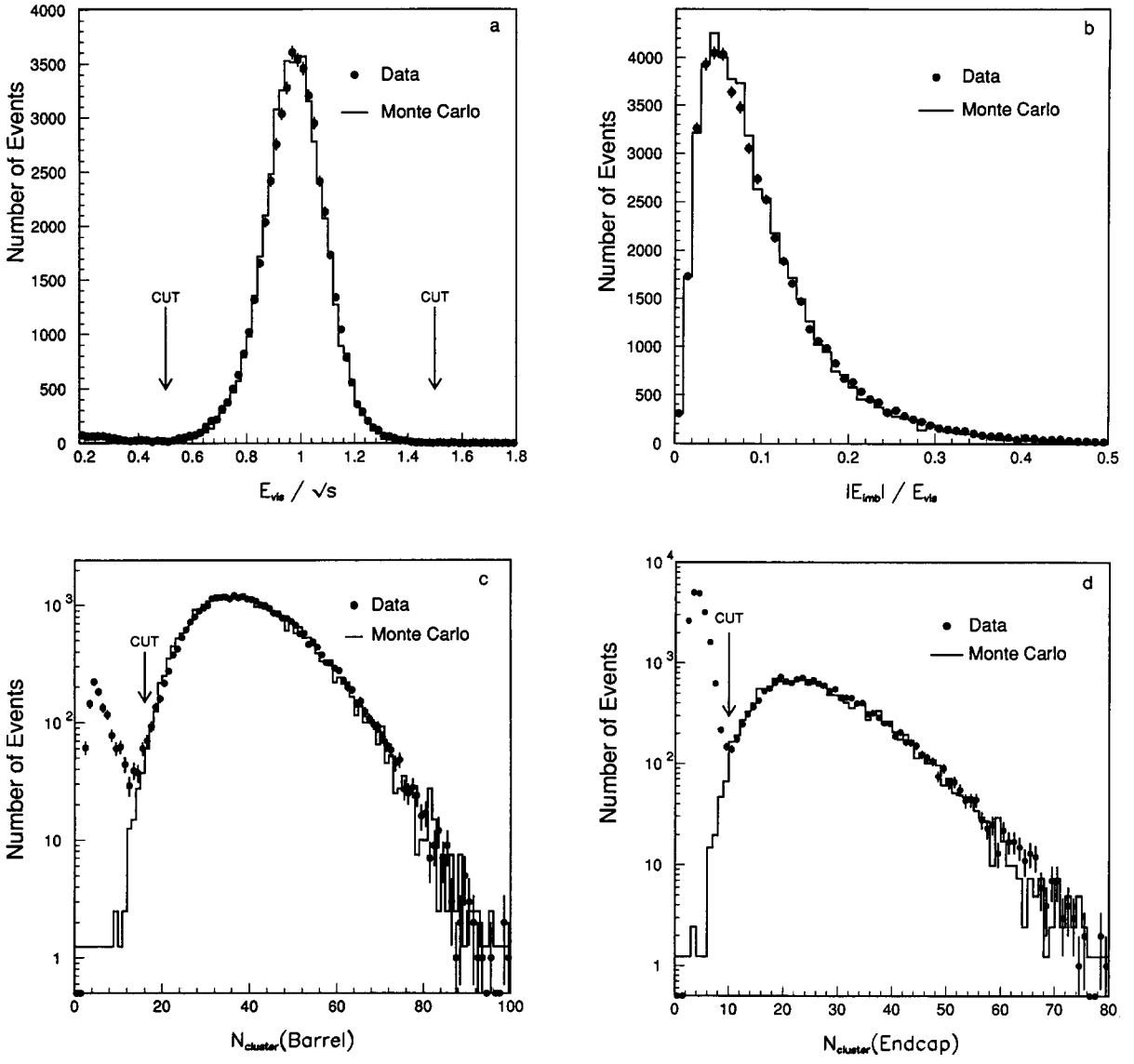

Fig. 3. (a) Distribution of the observed total energy E_{vis} normalized to $\sqrt{s}$ compared to the Monte Carlo simulation for hadron events. (b) Distribution of the observed total energy imbalance $|E_{imb}|$ normalized to the observed total energy E_{vis} compared with Monte Carlo. (c) Distribution of the observed number of energy clusters in the calorimeters $N_{cluster}$ compared with Monte Carlo for events where the polar angle of the thrust axis is larger than 42°. (d) Distribution of the observed number of energy clusters in the calorimeters $N_{cluster}$ compared with Monte Carlo for events where the polar angle of the thrust axis is smaller than 42°. The additional events in the data below the cut in (c) and (d) are due to $\tau^+\tau^-$ and e^+e^- production. The cuts used are indicated by the position of the arrows.

$M_Z = 91.164 \pm 0.013 \pm 0.030(\text{LEP})$ GeV,

$\Gamma_{\text{invisible}} = 0.502 \pm 0.018$ GeV,

$\chi^2/\text{DF} = 13.2/15$,

and with the standard model neutrino width of 0.167 GeV, we derive:

$N_\nu = 3.01 \pm 0.11$.

These values are in good agreement with previous re-

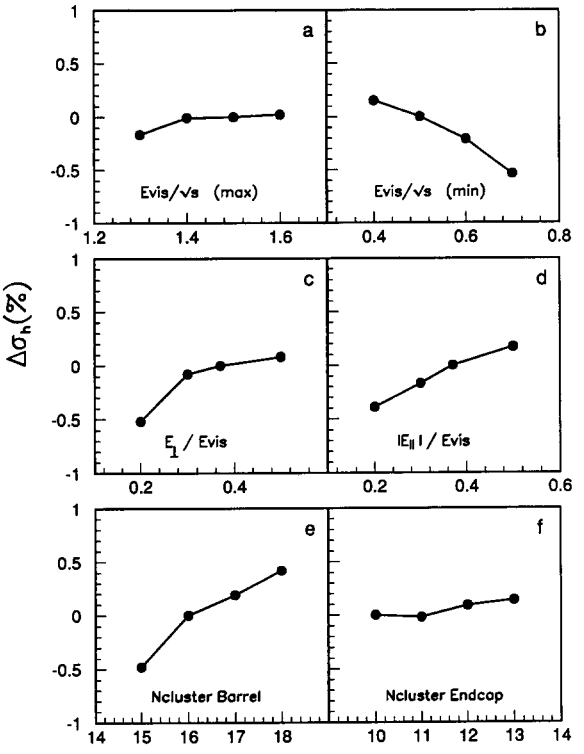

Fig. 4. The sensitivity to the cuts in fig. 3 (a) the maximum cut on the observed total energy E_{vis} normalized to $\sqrt{s}$, (b) the minimum cut on the observed total energy E_{vis} normalized to $\sqrt{s}$, (c) the cut on the observed energy imbalance perpendicular to the beam direction $E_\perp$ normalized to the total observed energy E_{vis}, (d) the cut on the observed energy imbalance parallel to the beam direction $E_\parallel$ normalized to the total observed energy E_{vis}, (e) the cut on the number of observed energy clusters in the calorimeters $N_{cluster}$ when the polar angle of the thrust axis is greater than 42°, and (f) the cut on the number of observed energy clusters in the calorimeters $N_{cluster}$ when the polar angle of the thrust axis is less than 42°.

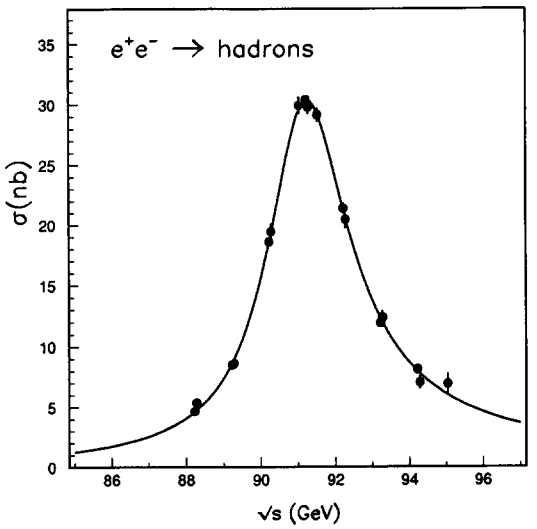

Fig. 5. The measured cross section for $e^+e^- \to$ hadrons as a function of $\sqrt{s}$. Data are shown with statistical errors only. The solid curve is a fit to the analytical forms [15–17] in which M_Z and $\Gamma_{invisible}$ were left free. The partial widths Γ_{ee} and Γ_h were taken from the standard model.

sults [2,3]. The fit and the data are shown in fig. 5.

The effect on the number of neutrino species of varying α_s, M_t and M_H has been studied. Varying these parameters in the range 0.105 to 0.125, 90 to 230 GeV and 40 to 1000 GeV, respectively, we find a change of $\Delta N_\nu = \pm 0.02$ around the central value of N_ν. The value of N_ν, when determined from this fit, is relatively insensitive to changes in these constants because the fit is dominated by the measurement of the peak cross section $\sigma_h^0 \propto (\Gamma_{ee}\Gamma_h)/\Gamma_Z^2$, where most of the variations in the widths cancel. A study of the effect of a point-to-point error on the central value of the beam energy, taking 0.010 GeV as an upper limit on the RMS value, leads to an additional error of ± 0.01 on N_ν.

We note that from our measured Z^0 mass, the value $\sin^2\theta_w = 0.2284 \pm 0.0043$ [19], and $40 < M_H < 1000$ GeV, we obtain [20] a value for M_t of 130^{+38}_{-42} GeV and an upper limit of 200 GeV (95% confidence level).

9. Simultaneous fit to hadron and muon data

We have also made a simultaneous fit to the hadron data and the data from $e^+e^- \to \mu^+\mu^-$ [21]. This fit is model independent with mass, width, hadronic width and leptonic width of the Z^0: M_Z, Γ_Z, Γ_h and $\Gamma_{\ell\ell}$ as free parameters. We have again used the analytical forms for the Z^0 cross sections given in refs. [15–17]. Systematic errors due to event selection for hadron and muon data are treated separately in the fit program, using an overall systematic error 1.4% from the luminosity measurement as discussed above. The results are summarized in table 2. We also give in table 2 some of the derived quantities after taking

Table 2
Results of simultaneous fit to hadron and muon data.

Parameter	Value	Standard model prediction
M_Z	$91.161 \pm 0.013 \pm 0.030$(LEP) GeV	
Γ_Z	2.492 ± 0.025 GeV	2.492 GeV
$\Gamma_{\ell\ell}$	0.0832 ± 0.0015 GeV	0.0838 GeV
Γ_h	1.748 ± 0.035 GeV	1.740 GeV
χ^2/DF	28.6/29	
from the above, the following quantities can be derived:		
$R_{had}=\Gamma_h/\Gamma_{\ell\ell}$	21.02 ± 0.62	20.77
$\Gamma_{invisible}$	0.494 ± 0.032 GeV	0.501 GeV
σ_h^{max}	41.38 ± 0.71 nb	41.46 nb
$\sigma_{\ell\ell}^{max}$	1.97 ± 0.06 nb	2.00 nb

into account the correlations between the fitted parameters (e.g. $\sigma_h^{max}=(12\pi/M_Z^2)\Gamma_{\ell\ell}\Gamma_h/\Gamma_Z^2$ is the maximum cross section with no radiative corrections). The standard model predictions are calculated using the central values of α_s, M_t and M_H as given above, and assuming $N_\nu=3$.

10. Mass limits on supersymmetric neutrinos

From the standard model fit we exclude the presence of any contributions to $\Gamma_{invisible}$ of more than 0.19 extra neutrino generations at the one-sided 95% confidence level. This can be used to impose limits on the mass of a stable spin-zero supersymmetric partner of the neutrino, $\tilde{\nu}$ [22]. If we assume that the 0.19 contribution is 100% due to this source with one $\tilde{\nu}$ contributing

$$\Delta N_\nu = \frac{1}{2}\left(1-\frac{4M_{\tilde{\nu}}^2}{M_Z^2}\right)^{3/2}$$

of one standard neutrino generation to the invisible width of the Z^0 [23], we exclude the existence of a $\tilde{\nu}$ with mass less than 31.4 GeV at the 95% confidence level. Assuming three degenerate $\tilde{\nu}$ families, we would find $M_{\tilde{\nu}} > 39.4$ GeV at the 95% confidence level.

Acknowledgement

We wish to thank CERN for its hospitality and help. We particularly express our gratitude to the LEP division: it is their excellent achievements which made this experiment possible. We thank the many engineers and technicians who constructed and maintain the experiment. We acknowledge the support of all the funding agencies which contributed to this experiment.

References

[1] S.L. Glashow, Nucl. Phys. 22 (1961) 579;
S. Weinberg, Phys. Rev. Lett. 19 (1967) 1264;
A. Salam, Elementary particle theory, ed. N. Svartholm (Almquist and Wiksell, Stockholm, 1968) p. 367.
[2] L3 Collab., B. Adeva et al., Phys. Lett. B 237 (1990) 136.
[3] ALEPH Collab., D. Decamp et al., Phys. Lett. B 235 (1990) 399;
DELPHI Collab., P. Abreu et al., Phys. Lett. B 241 (1990) 435;
MARK II Collab., G.S. Abrams et al., Phys. Rev. Lett. 63 (1989) 2173;
OPAL Collab., M.Z. Akrawy et al., Phys. Lett. B 240 (1990) 497.
[4] L3 Collab., B. Adeva et al., Nucl. Instrum. Methods A 289 (1990) 35.
[5] M. Böhm, A. Denner and W. Hollik, Nucl. Phys. B 304 (1988) 687;
F.A. Berends, R. Kleiss and W. Hollik, Nucl. Phys. B 304 (1988) 712.
[6] GEANT Version 3.13 (September 1989), see R. Brun et al., GEANT 3, CERN report DD/EE/84-1 (Revised) (September 1987);
the GHEISHA program is used to simulate hadronic interactions, see H. Fesefeldt, RWTH Aachen preprint PITHA 85/02 (1985).

[7] R. Kleiss and F.A. Berends, Nucl. Phys. B 186 (1981) 22 (programs supplied to L3 Collab. by the authors).
[8] M. Caffo, E. Remiddi and F. Semeria in: Z Physics at LEP 1, CERN report CERN-89-08, eds. G. Altarelli et al., Vol. 1 (CERN, Geneva, 1989) p. 171.
[9] S. Jadach and B.F.L. Ward, BHLUMI, version 1.2, version 1.11;
see S. Jadach and B.F.L. Ward, Phys. Rev. D 40 (1989) 3582;
B.F.L. Ward, private communication;
R. Kleiss et al., in: Z physics at LEP 1, CERN report, eds. G. Altarelli et al., Vol. 3 (CERN, Geneva, 1989) p. 92.
[10] D.R. Yennie, S.C. Frautschi and H. Suura, Ann. Phys. 13 (1961) 379.
[11] T. Sjöstrand and M. Bengtsson, Comput. Phys. Commun. 43 (1987) 367;
T. Sjöstrand in: Z Physics at LEP 1, CERN report CERN-89-08, eds. G. Altarelli et al., Vol. 3 (CERN, Geneva, 1989) p. 143.
[12] L3 Collab., B. Adeva et al., Phys. Lett. B 241 (1990) 416.
[13] A. Hoffman, CERN, private communication.
[14] L3 Collab., B. Adeva et al., Phys. Lett. B 248 (1990) 464.
[15] R.N. Cahn, Phys. Rev. D 36 (1987) 2666.
[16] A. Borrelli et al., Nucl. Phys. B 333 (1990) 357.
[17] D. Bardin et al., Z. Physics at LEP 1, CERN report CERN-89-08, eds. G. Altarelli et al., Vol. 3 (CERN, Geneva, 1989); D. Bardin et al., Berlin-Zeuthen preprint PHE-89-19 (1989).
[18] G. Burgers, CERN preprint CERN-TH-5119/88; in: Z. Physics at LEP 1, CERN report CERN-88-06, eds. G. Alexander et al. (CERN, Geneva, 1988) p. 121.
[19] UA2 Collab. J. Alitti et al., Phys. Lett. B 241 (1990) 150;
CDF Collab., S. Errede, presentation at DPF meeting of APS (Houston, Texas, USA, January 1990);
CDHS Collab., H. Abramowicz et al., Phys. Rev. Lett. 57 (1986) 298;
A. Blondel et al., CERN preprint CERN-EP-89/101;
CHARM Collab., J.V. Allaby et al., Phys. lett. B 177 (1986) 446;
J.V. Allaby et al., Z. Phys. C 36 (1987) 611;
D. Froidvaux, Invited talk at Intern Conf. at Neutrino 90 (June 1990).
[20] J. Ellis and G. Fogli, Phys. Lett. B 232 (1989) 139.
[21] L3 Collab., B. Adeva et al., Phys. Lett. B (247) 473.
[22] Y.A. Golfand and E.P. Likhtman, JETP Lett. 13 (1971) 323;
D.V. Volkhov and V.P. Akulov, Phys. Lett. B 46 (1973) 109;
J. Wess and B. Zumino, Nucl. Phys. B 70 (1974) 39;
P. Fayet and S. Ferrara, Phys. Rep. 32 (1977) 249;
A. Salam and J. Strathdee, Fortschr. Phys. 26 (1978) 57.
[23] X. Tata, preprint UH-511-673-89, and references therein;
R. Barbieri et al., CERN report CERN-89-08, eds. G. Altarelli et al., Vol. 2 (CERN, Geneva, 1989) p. 109.